Effect of distal stenosis on the blood flow in right coronary arteries with serial stenoses

***†Biyue. Liu[1] and Dalin Tang[2]**

[1]Department of Mathematics, Monmouth University, USA.
[2] Department of Mathematical Sciences, Worcester Polytechnic Institute, USA

*Presenting and †Corresponding author: bliu@monmouth.edu

Abstract

Computer simulations of the blood flow in right coronary artery with two stenoses in the same arterial segment are carried out to investigate the interactions of serial stenoses, especially the effect of the distal stenosis. Various mathematical models are developed by varying the location of the distal stenosis. The numerical results show that the variation of the distal stenosis has significant impact on coronary hemodynamics, such as the pressure drop, the flow shifting, and the flow separation. Our simulations demonstrate that the distal stenosis has insignificant effect on the disturbed flow pattern in the upstream and across the proximal stenosis regions. In a curved artery segment with two moderate stenoses of the same size, the distal stenosis causes a larger pressure drop and a more disturbed flow field in post stenotic region than the proximal stenosis does. A distal stenosis located at a further downstream position causes a larger pressure drop and a stronger reverse flow.

Keywords: right coronary artery, serial stenoses, pressure drop, flow disturbance

1. Introduction

Atherosclerosis, a disease of large- and medium-size arteries, involves complex interactions between the artery wall and the blood flow. Hemodynamics plays an important role in the pathogenesis of atherosclerosis [1]-[5]. Vascular geometry is one of the risk factors strongly influencing the flow patterns and generating a pre-existing atherogenic hemodynamic environment [1][3]. Both clinical observations and experiment results show that there is a strong correlation between the sites of flow disturbance and preferential areas for the development of atherosclerotic diseases [2][4]. Atherosclerotic lesions originate preferably at the vessel branches, bifurcations and bends, where the blood vessel curvature creates dynamic environments of disturbed flow.

The obstruction presented by a moderate to severe stenosis can lead to a highly disturbed flow region at the downstream of the stenosis. The influence of an arterial stenosis in local blood flow is of considerable clinical importance. Many experimental and mathematical researches on hemodynamics in stenotic arteries have been reported to investigate the influence of the stenosis on the flow field downstream [6]-[9]. The presence of a moderate to severe stenosis significantly affects the downstream blood flow pattern, such as flow separation, secondary flow, low wall shear stress, and large pressure drop. These characteristic changes of the flow downstream may lead to the formation of a second stenosis [9]-[12]. In many clinical situations, the patient is found to have multiple stenoses in the same arterial segment.

The fluid dynamic interaction of multiple stenoses in coronary arteries is complex and cannot be adequately assessed by visual interpretation on the coronary angiogram [10]. The effect of serial stenoses on coronary hemodynamics has drawn much attention. Many researchers have conducted the experimental and clinical investigations [13]-[16] and the numerical simulations [11][18]-[24].The existence of multiple stenoses can cause a decrease in blood flow at each stenosis, and then the pressure gradient at each stenosis can be lower than that at the stenosis if it were a single lesion in a vessel [17]. The study of De Bruyne *et al.* demonstrated that for multiple stenoses in the same vessel, the hemodynamic assessment of a stenosis and the potential benefit of angioplasty is significantly influenced by the presence of the second stenosis [25]. Talukder *et al.* showed that the total pressure drop across a series of mild stenoses increases linearly as the number of stenoses increases [16]. Using *in-vitro* experiments, D'Souza *et al.* found that the pressure drop coefficient of the upstream stenosis varies insignificantly in the presence of a downstream stenosis with a varying degree of severity [13]. Lee *et al.* performed numerical simulations of turbulent flow through tubes with double stenoses. They found that the maximum centerline velocity and disturbance intensity at the second stenosis are higher than those at the first stenosis when both stenoses have a 50% area reduction. The downstream stenosis usually does not have perceptible influences on the upstream flow fields [19][20].

In literature all of the numerical simulations examining the effect of multiple stenoses with varying size/location were performed using 2D models of axisymmetric straight tube. However, not much work has been reported on the effect of multiple stenoses on blood flow in curved arteries. No systematic study of the fluid dynamics of multiple stenoses in a segment of curved artery has been reported previously in the literature. It is expected that the curvature of the artery may intensify the complex of the blood flow in arteries with serial stenoses. In the present study, the blood flows in right coronary arteries with two stenoses are numerically examined. The coronary artery models are constructed based on the angiographic image of a patient with altered location of the stenoses.

2. Mathematical Models and Method

In the present study, the blood is assumed to be a laminar, incompressible, and non-Newtonian viscous fluid obeying the Carreau model [26][27]. The blood density ρ is assumed to be a constant at 1050 kg/m^3. The geometries of the models are constructed based on the inlet and outlet diameters and the center-line curve of the angiographic image of the coronary segment of a patient (see [28]), with varying locations of two moderate stenoses. The stenotic artery segments are 5.25*cm* in length with a diameter of 0.3256*cm* and 0.2954*cm* at the inlet and the outlet, respectively. In the computer simulation, to reduce the influence of the boundary conditions in the region of interest each coronary artery segment is extended at the inlet and the outlet by 0.6*cm* and 0.8*cm*, respectively. Including the extended inlet and outlet, the total length of coronary artery segment is 6.65cm in each model. At the inlet boundary, a time dependent pressure with waveform *Pin* (see Fig. 1) and a no-viscous-stress condition are applied. At the outlet boundary, a fully developed velocity profile with pulse waveform (see *Vout* in Fig. 1) is imposed as a normal outflow velocity. The pressure and the velocity waveforms in Fig.1 were extracted from the on-site blood pressure and flow velocity data of the patient [27][28]. A normalized time length t/t_p = 1 is used for simplicity. On the artery wall a non-slip boundary condition is imposed.

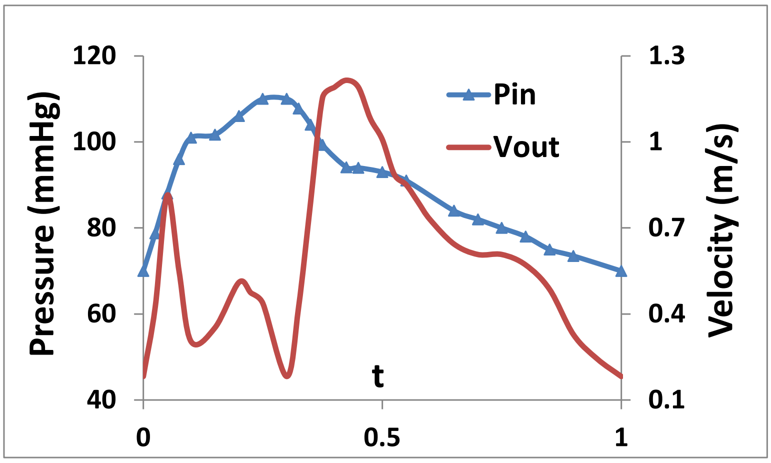

Figure 1. velocity and pressure waveforms

Unsteady Navier-Stokes equations are solved numerically with the finite element method over unstructured tetrahedral elements. The computations are performed using COMSOL 5.2a. To confirm that the numerical solutions are independent of the spatial mesh, the computations are repeated over the refined meshes till the maximum relative errors of the blood pressure over two consecutive refined meshes is less than 0.5%. Computations are performed over four consecutive cardiac cycles to ensure a truly periodic flow. The maximum relative error of the blood pressure between the third and the forth cycles is 0.53%. All numerical results presented in this paper are obtained over the meshes with about 2760000 elements.

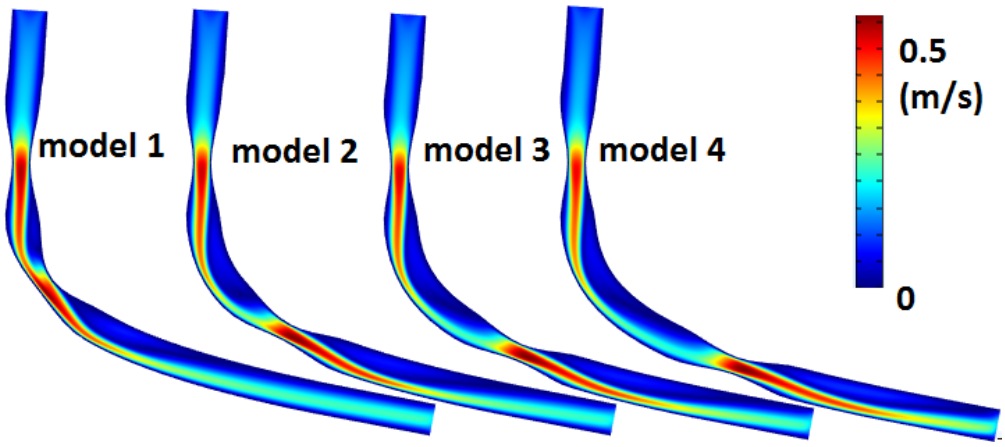

Figure 2. Magnitude of velocity at the center plane when t = 0.3 for four models

3. Numerical Results and Discussions

The shape of the stenotic coronary arteries and the location of stenoses are clearly shown in Fig. 2, including the extended inlet and outlet. The location of the proximal stenosis is the same in all four coronary models while the location of the distal stenosis is different in each model. The inter-stenotic distance between the necks of the proximal and the distal stenoses is 1.22*cm* (~3.9D), 1.96*cm* (~6.3D), 2.32*cm* (~7.5D), and 2.69*cm* (~8.7D) for model 1 through model 4, respectively. Here D is the average diameter of the artery. Both proximal and distal stenoses have the same length of 0.98*cm*, and a cross-section area reduction of 75% at the neck.

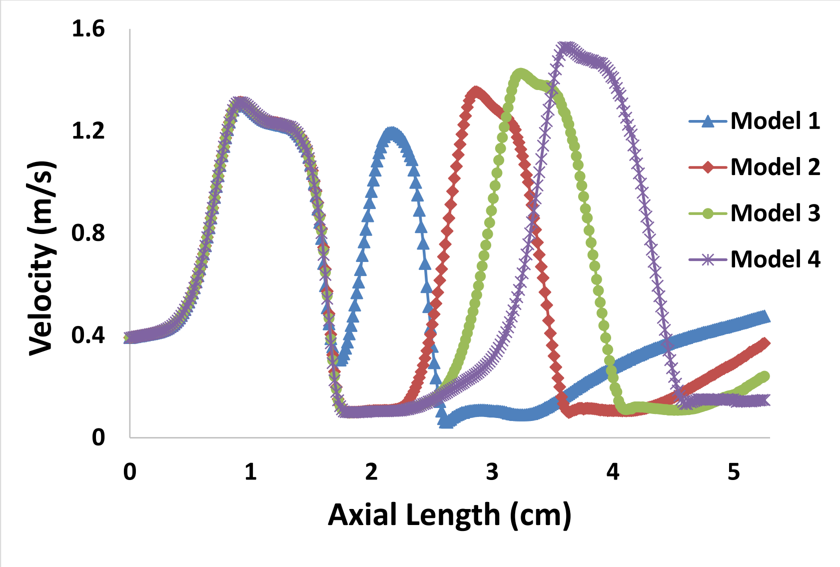

Figure 3. Temporal mean velocity magnitude along the center line of artery

Figure 2 plots the contour of velocity magnitude along the center plane for each coronary model at t = 0.3. Figure 3 plots the temporal mean velocity magnitude along the center line of the artery for each model. The horizontal axis is the axial length with z = 0*cm* and 5.25*cm* as the real inlet and outlet, respectively (The extended inlet and outlet are not included in Fig. 3). The neck of the proximal stenosis is at z = 0.86*cm* for all four models. The neck of the distal stenosis is at z = 2.08*cm*, 2.81*cm*, 3.18*cm* and 3.54*cm* for model 1, model 2, model 3 and model 4, respectively. Figure 4 includes the velocity field in the center plane of the artery at t = 0.8 for each model, including the extended inlet and outlet. Figure 5 is the plot of the slice-averaged PD_{mean} from the inlet to the outlet of the artery. Here PD_{mean} is the temporal mean pressure drop. A total of 128 points are picked evenly spaced on the lumen boundary of each cross-section. The PD_{mean} is averaged on the picked points of each slice.

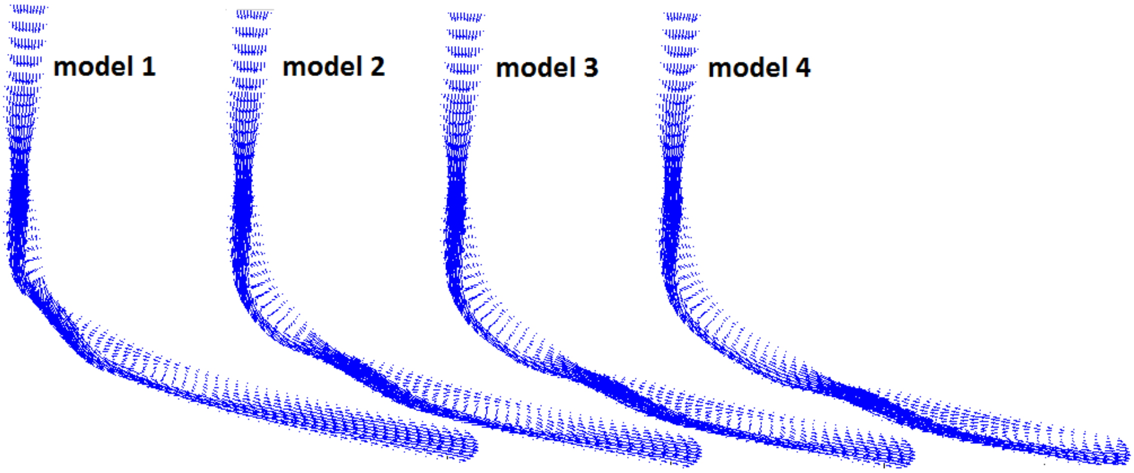

Figure 4. Plots of velocity field along the center plane at t = 0.8.

Flow Shifting

The contour plot of the velocity magnitude along the center plane for each model in Fig. 2 shows the pattern of flow shifting in right coronary artery with two moderate stenoses of the same size. For models 2-4, the flow shifting in the stenotic area and post-stenotic area of the proximal stenosis is identical. This indicates that the location of the distal stenosis has no effect on the flow shifting pattern of the proximal stenosis when the inter-stenotic distance is six times the diameter of the artery or greater. In addition, we can also see that the flow shifting in the post stenotic region of the distal stenosis is stronger than that in the proximal stenosis even though both stenoses have the same severity. This observation can also be confirmed quantitatively by Fig. 3. The velocity magnitude along the center line is the same between z = 0*cm* (the inlet) and z = 2.32*cm* (the front edge of the distal stenosis of model 2) for models 2-4. The peak value at the neck of the distal stenosis is higher than that at the neck of the proximal stenosis for models 2-4. The further down the location of the distal stenosis, the higher of the velocity at the neck of the distal stenosis. The above discussed behaviors do not apply to model 1, where the flow shifting following the distal stenosis is weaker. This is probably due to the fact that the existence of the proximal stenosis will affect the flow disturbance of the stenosis in downstream when two stenosis are too close.

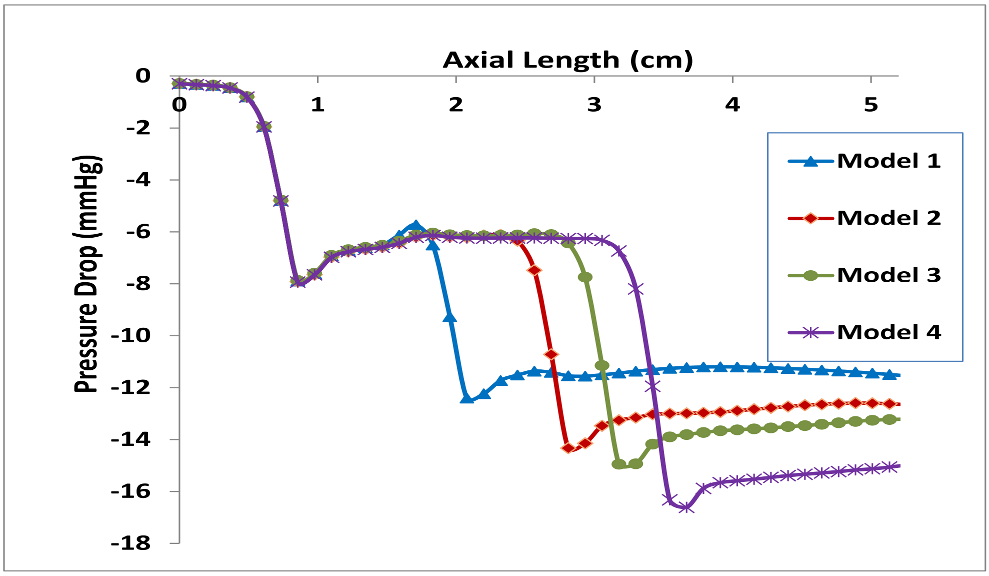

Figure 5. Slice averaged temporal mean pressure drop along the artery

Flow Separation

The formation and progression of a flow separation zone is one of the most important flow phenomena in the post stenosis region. Stenosis severity is strongly associated with the recirculation zone. The response of vascular endothelium to disturbed flow and its role in the pathogenesis of atherosclerosis have been studied extensively [29][30]. A net migration is directed away from the region of high shear gradient in a disturbed flow field. Following the reverse flow within the recirculation zone, the particle is exposed to low shear stress levels for a relative prolonged duration [30][31]. Figure 4 demonstrates the flow separation patterns in coronary arteries with two stenoses. In the post-stenosis area of each stenosis there is a region of flow separation near the inner wall of the bend. Comparing these two regions in each of the model plotted in Fig. 4, we can see that the distal stenosis results in a larger area of the flow separation and a stronger reverse flow near the inner wall. The further downstream the distal stenosis locates, the larger the area of the flow separation it results. It is evident that having the same area reduction the distal stenosis is more hemodynamically significant than the proximal stenosis in a right coronary artery segment with two stenoses.

Pressure Drop

The blood pressure difference along the coronary arterial length is one of the important initiating factors for atherosclerosis and intimal hyperplasia development [32]. The magnitude of the pressure drop has been clinically used to judge severity of the lesion. Several popularly used diagnostic parameters assessing the functionally significance of a stenosis are related to the pressure drop across the stenosis, such as the fractional flow reserve (*FFR*) and the pressure drop coefficient (*CDP*). Therefore it is of practical interest to examine the pressure drop pattern in coronary arteries with serial stenoses when investigating the effect of the distal stenosis. The curves of the slice averaged temporal mean pressure drop along the axial artery length plotted in Fig. 5 demonstrate that the distal stenosis does not affect the pressure drop across the proximal stenosis. On the other hand, the pressure drop across the distal stenosis could be influenced by the proximal stenosis if two stenoses are too close. When the inter-stenotic distance is six times the diameter of the artery or greater the pressure drop across the distal stenosis is larger than that across the proximal stenosis even though both stenoses have the same size of area reduction. A distal stenosis located in a further downstream position causes a larger pressure drop.

4. Conclusions

In this study coronary models are developed to investigate the hemodynamics of blood flows in right coronary artery segments with serial stenoses and to examine the effect of the distal stenosis. The center line of the artery segment and the location of the proximal stenosis are based on the angiographic image of the coronary segment of a patient, while the location of the distal stenosis varies in different models. Both stenoses are moderate with a 75% reduction in cross section area. Our simulations show that when the inter-stenotic distance is greater than or equal to six times the diameter of the artery the distal stenosis has insignificant effect on blood flow behavior from the inlet to the post-stenotic region of the proximal stenosis, such as the flow shifting pattern, the magnitude of velocity along the center line, the pressure drop, the area of flow recirculation and the strength of the reverse flow. In a right coronary artery segment with two moderate stenoses of the same size, the distal stenosis causes a more disturbed flow in the post stenotic region. Compared with those of the proximal stenosis, the flow shifting in the post stenotic region of the distal stenosis is stronger, the flow separation area downstream of the distal stenosis is larger, and the pressure drop across the distal stenosis is larger. The further downstream the distal stenosis locates, the more disturbed flow it creates in the post stenotic region. In summary, when two stenoses have the same size, the distal stenosis is more hemodynamically significant.

Acknowledgement. This work is partially supported by a grant from the Simons Foundation (#210082 to Biyue Liu), NIH grant NIH/NIBIB R01 EB004759, and a Jiangsu Province Science and Technology Agency grant BE2016785.

References

[1] Friedman, M.H., Hutchins, G.M., Bargeron, C.B., Deters, O.J., Mark, F.F. (1981) Correlation between intimal thickness and fluid shear in human arteries, *Atherosclerosis* **39**, 425–436.

[2] Karino, T. (1986) Microscopic structure of disturbed flows in the arterial and venous systems, and its implication in the localization of vascular diseases, *International Angiology: A Journal of the International Union of Angiology* **4**, 297–313.

[3] Myers, J.G., Moore, J.A., Ojha, M., Johnston, K.W., Ethier, C.R. (2001) Factors influencing blood flow patterns in the human right coronary artery, *Ann Biomed Eng* **29**, 109–20.

[4] Ku, D.N., Giddens, D.P., Zarins, C.K., Glagov, S. (1985) Pulsatile flow and atherosclerosis in the human carotid bifurcation: positive correlation between plaque location and low and oscillating stress, *Arteriosclerosis* **5**, 292–302.
[5] Prosi, M., Perktold, K., Ding, Z., Friedman, M.H. (2004) Influence of curvature dynamics on pulsatile coronary artery flow in a realistic bifurcation model, *J Biomech* **37**, 1767–75**.**
[6] Long, Q., Xu, X.Y., Ramnarine, K.V., Hoskins, P. (2001) Numerical investigation of physiologically realistic pulsatile flow through arterial stenosis, *J Biomech* **34**,1229–42.
[7] Stroud, J.S., Berger, S.A., Saloner, D. (2000) Influence of stenosis morphology on flow through severely stenotic vessels: implications for plaque rupture, *J Biomech* **33**, 443–55.
[8] Nosovitsky, V.A., Ilegbusi, O.J., Jiang, J., Stone, P.H., Feldman, C.L. (1997) Effects of curvature and stenosis-like narrowing on wall shear stress in a coronary artery model with phasic flow, *Comput Biomed Res* **30**, 61–82.
[9] Liu, B. (2007) The influences of stenosis on the downstream flow pattern in curved arteries. *Medical engineering & physics* **29(8)**, 868-876.
[10] Bernad, S.I., Bernad, E.S., Craina, M., Sargan, I., Totoran, A., Brisan, C. (2012) Particle Depositions and Related Hemodynamic Parameters in the Multiple Stenosed Right Coronary Artery, *J Clin Med Res* **4(3)**, 177-189.
[11] Bernad, S.I., Bernad, E.S., Totorean, A.F., Craina, M.L., Sargan, I. (2015) Clinical important hemodynamic characteristics for serial stenosed coronary artery, *Int. J. of Design & Nature and Ecodynamics.* **10**, 97–113.
[12] Dash, R.K., Jayaraman, G., Mehta, K.N. (1999) Flow in a catheterized curved artery with stenosis, *J Biomech* **32**, 49–61.
[13] D'Souza, G.A., Peelukhana, S.V., Banerjee, R.K. (2014) Diagnostic Uncertainties During Assessment of Serial Coronary Stenoses: An In Vitro Study, *Journal of Biomechanical Engineering* **136**, 021026-1-11**.**
[14] Pijls, N.H.J. De Bruyne, B., Bech, G.J.W., Liistro, F., Heyndrickx, G.R., M.Bonnier, H.J.R., Koolen, J.J. (2000) Coronary Pressure Measurement to Assess the Hemodynamic Significance of Serial Stenoses Within One Coronary Artery: Validation in Humans, *Circulation* **102**, 2371–2377.
[15] Sabbah, H.N., Stein, P.D. (1982) Hemodynamics of multiple versus single 50 percent coronary arterial stenoses, *Am. J. Cardiol* **50**, 276–280.
[16] Talukder, N., Karayannacos, P.E., Nerem, R.M., Vasko, J.S. (1977) An experimental study of the fluid dynamics of multiple noncritical stenoses, *J. Biomech. Eng.* **99**, 74–82
[17] Tanaka, K., Bezerra, H.G., Gaur, S., Attizzani, G.F., Botker, H.E., Costa, M.A., Rogers, C., Norgaard, B.L. (2015) Comparison Between Non-invasive (Coronary Computed Tomography Angiography Derived) and Invasive-Fractional Flow Reserve in Patients with Serial Stenoses Within One Coronary Artery: A NXT Trial substudy, *Annals of Biomedical Engineering*, **44**, 580–589.
[18] Bertolotti, C., Qin, Z., Lamontagne, B., Durand, L.G., Soulez, G., Cloutier, G. (2006) Influence of multiple stenoses on echo-Doppler functional diagnosis of peripheral arterial disease: a numerical and experimental study, *Ann. Biomed. Eng.* **34**, 564–574.
[19] Lee, T.S., Liao, W., Low, H.T. (2003) Numerical simulation of turbulent flow through series stenoses, *Int. J. Numer. Meth. Fluids* **42,** 717–740.
[20] Lee T.S., Liao W., Low, H.T. (2004) Numerical study of physiological turbulent flows through series arterial stenoses, *Int. J. Numer. Meth. Fluids* **46**, 315-344.
[21] Mustapha, N., Amin, N., Chakravarty, S., Mandal, P.K. (2009) Unsteady magnetohydrodynamic blood flow through irregular multi-stenosed arteries, *Comput. Biol. Med*. **39**, 896-906.
[22] Park, S.J., Ahn, J.-M., Pijls, N.H.J., et al, (2012) Validation of Functional State of coronary Tandem Lesions Using Computational Flow Dynamics," *Am. J. Cardiol,* **110**1578–1584.
[23] Jahangiri, M., Saghafian, M., Sadeghi, M.R. (2015) Numerical simulation of hemodynamic parameters of turbulent and pulsatile blood flow in flexible artery with single and double stenoses, *Journal of Mechanical Science and Technolog*y **29**, 3549~3560.
[24] Liu, B. Zheng, J., Bach R., Tang D. (2017) Influences of Flow Parameters on Pressure Drop in a Patient Specific Right Coronary Artery with Two Stenoses, *Computational Science and Its Application – ICCSA 2017*, Part I, LNCS 10404, Springer (to appear).
[25] De Bruyne, B., Pijls, N.H.J., Heyndrickx, G.R., Hodeige, D., Kirkeeide, R., Gould, K.L. (2000) Pressure-Derived Fractional Flow Reserve to Assess Serial Epicardial Stenoses Theoretical Basis and Animal Validation, *Circulation*. **101**, 1840-1847.
[26] Cho, Y.I., Kensey, K.R. (1991) Effects of the non-Newtonian viscosity of blood on flows in a diseased arterial vessel. Part 1: steady flows, *Biorheology* **28**, 241-262.
[27] Liu, B., Zheng, J., Bach, R., Tang D. (2015) Influence of model boundary conditions on blood flow patterns in a patient specific stenotic right coronary artery, *BioMedical Engineering OnLine* **14**(Suppl 1):S6
[28] Fan, R., Tang, D., Yang, C., Zheng, J., Bach, R., Wang, L., Muccigrosso, D., Billiar, K., Zhu, J., Ma, G., Maehara, A., Mintz, G.S. (2014): Human coronary plaque wall thickness correlated positively with flow

shear stress and negatively with plaque wall stress: an IVUS-based fluid-structure interaction multi-patient study, *BioMedical Engineering OnLine* 13:32.
[29] Traub, O., Berk, B.C. (1998) Laminar shear stress mechanics by which endothelial cells transducer an atheroprotective force, *Arterioscler Thromb Vasc Biol* **18**, 677-685.
[30] Tardy, Y., Resnick, N., Nagel, T, (1997) Gimbrone MA Jr, Dewey CF Jr. Shear stress gradients remodel endothelial monolayers in vitro via a cell proliferation-migration-loss cycle, *Arterioscler Thromb Vasc Biol* **17**, 3102-3106.
[31] Raz, S., EINAV, S., ALEMU, Y., BLUESTEIN, D. (2007) DPIV prediction of flow induced platelet activation – comparison to numerical predictions, *Annals of Biomedical Engineering* **35**, 493-504.
[32] Giannoglou, G.D., Soulis, J.V., Farmakis, T.M., Giannakoulas, G.A., Parcharidis, G.E., Louridas, G.E. (2005): Wall pressure gradient in normal left coronary artery tree. *Medical Engineering & Physics* 27, 455–464.